

The Evolution of the Pion Distribution Amplitude in Next-to-Leading Order

D. Müller

Stanford Linear Accelerator Center,
Stanford University, Stanford, California 94309

Abstract

The evolution of the pion distribution amplitude in next-to-leading order is studied for a fixed and a running coupling constant. In both cases, the evolution provides a logarithmic modification in the endpoint region. Assuming a simple parameterization of the distribution amplitude at a scale of $Q_0 \sim 0.5$ GeV, it is shown numerically that these effects are large enough at $Q \sim 2$ GeV that they have to be taken into account in the next-to-leading-order analysis for exclusive processes. Alternatively, by introducing a new distribution amplitude that evolves more smoothly, this logarithmic modification can be included in the hard-scattering part of the considered process.

1 Introduction

The perturbative approach for hard exclusive quantum chromodynamic (QCD) processes was developed for more than one decade [1, 2, 3, 4] (see Ref. [5] for reviews). In this approach, the scattering amplitude at large momentum transfer Q^2 factorizes as a convolution of process-independent distribution amplitudes, with a process-dependent perturbatively computable hard-scattering amplitude. By using the leading-order perturbative QCD (pQCD) analysis, which was performed for a large number of exclusive processes including mesons and baryons, the qualitative behavior for large Q^2 could be well understood [6, 7]. However, using the asymptotic distribution amplitudes, which follow directly from the solution of the evolution equation, results in predicted normalizations for the elastic form factors at experimental accessible momentum transfer that are too small; in the case of the magnetic nucleon form factor, this provides the opposite sign.

From deep inelastic scattering, where the application of pQCD is generally accepted, it is known that the used parton distribution functions for accessible Q^2 are far from their asymptotic form where all higher moments m_n , i.e., $n > 0$, vanish. It is therefore expected that for the exclusive processes at accessible momentum transfer, the distribution amplitudes are nonasymptotical. Choosing distribution amplitudes that are enhanced in the endpoint region (and asymmetric for nucleons) provides the observed normalization and sign for the elastic form factors.

Reference [8] argues that choosing such enhanced amplitudes provides inconsistencies that affect the importance of higher twist contributions, as well as of perturbative nonleading-order terms, and so the pQCD approach to elastic form factors probably is not self-consistent. (A second point widely discussed in the literature is the nonperturbative contribution from the hadronic wave function [8, 9].) Phenomenological methods, such as (1) introduce a gluon mass, (2) freeze the running coupling constant for small virtuality [10], or (3) suppress the endpoint region by suitable distribution amplitudes or by a cutoff [11], are used to improve the stability of the pQCD approach. Recent incorporation of Sudakov suppression has shown that the pQCD approach for the pion form factor is self-consistent for a momentum transfer of $Q \sim 20\Lambda_{QCD}$ [12] (see also Ref. [13]).

The validity of the pQCD approach for exclusive processes can also be studied by direct calculations of higher twist and perturbative nonleading contributions. It appears that higher twist analyses have not been achieved quantitatively. The stability of the perturbation theory has been investigated neglecting the evolution of the distribution amplitude by next-to-leading-order calculations for the pion transition form factor Ref. [14, 15], the pion form factor [16, 17], and the two-photon processes $\gamma\gamma \rightarrow M^+M^-$ ($M = \pi, K$) [18]. Discrepancies in the one-loop approximation of the hard-scattering amplitude for the pion form factor were clarified in Ref. [19, 20]. The next-to-leading-order correction to the pion form factor and to the processes $\gamma\gamma \rightarrow M^+M^-$ are rather large at accessible momentum transfer.

Including the evolution of the distribution amplitude in these analyses requires the solution of the differential-integral evolution equation, which can be done by using the moment method. The corresponding two-loop approximation of the integral kernel was computed by different authors and the obtained results agree with each other [21]. It has been confirmed that the computed evolution kernel is consistent with the Gribov-Lipatov-Altarelli-Parisi kernel [22] and with conformal symmetry breaking in massless gauge field theories [23]. Because of the complicated structure of the evolution kernel, only the first few moments of the evolution kernel had been computed numerically [24]. Based on this incomplete computation, it was believed that the next-to-leading-order correction to the evolution of the distribution amplitude and the contribution of this correction to the pion form factor are rather small [24, 25].

Recently, using conformal constraints, the complete formal solution of the evolution equation in next-to-leading order could be obtained without knowing the evolution kernel by a one-loop calculation [23]. This paper studies this solution in detail and shows that the evolution of the distribution amplitude must be included in the next-to-leading order analysis. Section 2 reviews to leading order the evolution equation of the distribution amplitude and the solution in terms of the conformal spin expansion. The evolution of the distribution amplitude in next-to-leading order for fixed α_s is studied in Section 3. This includes a detailed investigation of the large n behavior for the next-to-leading order corrections to the eigenfunctions $\varphi_n^{ef}(x, \alpha_s)$ and eigenvalues $\gamma_n(\alpha_s)$ of the evolution kernel. Numerical results for the evolution of the asymptotic, the Chernyak-Zhitnitsky two-hump, and another convex distribution amplitude are presented. Section 4 analyzes the solution of the evolution equation in next-to-leading order with running coupling, showing by numerical computation that the next-to-leading-order corrections are also large in this case. Section 5 discusses the obtained result, comparing it with a previous result [24], and presents the conclusions.

2 The Distribution Amplitude and their Evolution

The distribution amplitude $\varphi(x, Q^2)$ is the probability amplitude for finding a valence quark [antiquark] with light cone momentum fraction x [$1 - x$] in the pion probed at large momentum square Q^2 [1]. This amplitude can be defined as expectation value of renormalized nonlocal light cone operators [1, 22]

$$\varphi(x, Q^2) = f_\pi^{-1} \int \frac{d\kappa}{\pi} \exp[i\kappa(\tilde{n}P)(2x - 1)] \langle 0|O(\kappa; \tilde{n})|P \rangle \Big|_{\mu^2 = Q^2} , \quad (1)$$

where for simplicity, the renormalization point μ^2 is set equal to the large momentum transfer Q^2 (this choice is not optimal with respect to the factorization scale setting for the considered processes; however, it is sufficient for the following discussions). The light ray vector \tilde{n} is chosen as $\tilde{n} = (\tilde{n}_+ = 0, \tilde{n}_- = 2, \vec{0}_\perp)$ so that $\tilde{n}P = P_+$, $|P\rangle$ denotes the pion state with momentum P , and

$$O(\kappa; \tilde{n}) = :\bar{\psi}_d(-\kappa\tilde{n}) \gamma_5(\tilde{n}\gamma) U(-\kappa\tilde{n}, \kappa\tilde{n}) \psi_u(\kappa\tilde{n}): \quad (2)$$

is the light-cone operator with the flavor content of the considered pion. The path ordered phase factor $U(-\kappa\tilde{n}, \kappa\tilde{n})$ ensures the gauge invariance of this operator. The pion decay constant $f_\pi = 133$ MeV introduced in (1) guarantees the normalization [1]

$$\int_0^1 dx \varphi(x, Q^2) = f_\pi^{-1} \langle 0|:\bar{\psi}_d(0) \gamma_5(\tilde{n}\gamma) \psi_u(0):|P \rangle / \tilde{n}P = 1 . \quad (3)$$

Analogous to a quantum mechanical ground state, it is to be expected that $\varphi(x, Q^2)$ can be chosen positive. Notice that because of charge conjugation invariance, the symmetry relation $\varphi(x, Q^2) = \varphi(1 - x, Q^2)$ holds true.

The evolution equation for $\varphi(x, Q^2)$ derived in Ref. [1, 6] can also be obtained in a straightforward manner from the renormalization group equation of the nonlocal operator $O(\kappa; \tilde{n})$ [22]

$$Q^2 \frac{d}{dQ^2} \varphi(x, Q^2) = \int_0^1 dy V(x, y; \alpha_s(Q^2)) \varphi(y, Q^2) , \quad (4)$$

where $\alpha_s = g^2/(4\pi)$ is the QCD fine structure constant. The evolution kernel $V(x, y; \alpha_s) = (\alpha_s/2\pi) V^{(0)}(x, y) + (\alpha_s/2\pi)^2 V^{(1)}(x, y) + \dots$ has been computed perturbatively in one- and two-loop approximation by using the dimensional regularization in the modified minimal subtracted $\overline{\text{MS}}$ -scheme [21].

The evolution equation (4) can be solved by conformal spin expansion

$$\varphi(x, Q^2) = \sum_{n=0}^{\infty} \frac{(1-x)x}{N_n} C_n^{3/2}(2x-1) \langle 0|O_n(\mu^2)|P \rangle^{\text{red}} \Big|_{\mu^2 = Q^2} , \quad (5)$$

$$N_n = \frac{(n+1)(n+2)}{4(2n+3)} ,$$

where the sum runs only over even n [to ensure the above mentioned symmetry of $\varphi(x, Q^2)$]. Here, $\langle 0|O_n(Q^2)|P \rangle^{\text{red}} = \int_0^1 dx C_n^{3/2}(2x-1)\varphi(x, Q^2)$ are reduced expectation values of local

operators that in leading order do not mix under renormalization [3, 26]. In the free field theory, these operators labeled by the conformal spin form an infinite irreducible representation of the so-called collinear conformal algebra, which is a subalgebra $O(2, 1)$ of the full conformal algebra $O(4, 2)$ [27]. The Gegenbauer polynomials $C_n^{3/2}$ of order 3/2 form an orthogonal and complete basis in the space of quadrate integrable functions with the weight $(1-x)x$. Thus, expansion (5) converges if $\varphi(x, Q^2)$ vanishes at the endpoints of the interval $[0, 1]$; see, for instance, Ref. [28]. This condition is automatically satisfied [6].

The Q -dependence of $\langle 0|O_n(Q^2)|P \rangle^{\text{red}}$ can be determined from the evolution equation

$$Q^2 \frac{d}{dQ^2} \langle 0|O_n(Q^2)|P \rangle = \frac{1}{2} \sum_{k=0}^{n'} \gamma_{nk}(\alpha_s(Q^2)) \langle 0|O_k(Q^2)|P \rangle , \quad (6)$$

where the anomalous dimension matrix $\gamma_{nk} = (\alpha_s/2\pi) \gamma_n^{(0)} \delta_{nk} + (\alpha_s/2\pi)^2 \gamma_{nk}^{(1)} + \dots$ is diagonal in one-loop order. In general, Poincaré-invariance of the theory assures the triangularity of the matrix $\hat{\gamma} := \{\gamma_{nk}\}$. The eigenvalues $\gamma_n = \gamma_{nn}$ are identical with the flavor nonsinglet anomalous dimensions known from deep inelastic scattering (moments of the Gribov-Lipatov-Altarelli-Parisi kernel). In leading order the solution of (6) is given by

$$\langle 0|O_n(Q^2)|P \rangle = \left(\frac{\alpha_s(Q_0^2)}{\alpha_s(Q^2)} \right)^{\gamma_n^{(0)}/\beta_0} \langle 0|O_n(Q_0^2)|P \rangle , \quad (7)$$

$$\alpha_s(Q^2) = \frac{4\pi}{\beta_0 \ln(Q^2/\Lambda^2)} ,$$

where Q_0 is an appropriate reference momentum, Λ is the QCD scale parameter,

$$\gamma_n^{(0)} = C_F \left[3 + \frac{2}{(n+1)(n+2)} - 4 \sum_{i=1}^{n+1} \frac{1}{i} \right] , \quad (8)$$

$C_F = 4/3$ and $\beta_0 = (11/3) C_A - (2/3) n_f$, with n_f is the number of active quarks and $C_A = 3$.

Since $\gamma_n^{(0)} < 0$ for $n > 0$, $\langle 0|O_n(Q^2)|P \rangle^{\text{red}}$ decrease [see Eq. (7)] with increasing Q^2 , so that all harmonics with $n > 0$ will also be suppressed. Furthermore, current conservation implies $\gamma_0^{(0)} = 0$ so that from Eq. (5) the asymptotic distribution amplitude follows:

$$\varphi^{as}(x) = \lim_{Q^2 \rightarrow \infty} \varphi(x, Q^2) = 6(1-x)x , \quad (9)$$

which does not evolve in leading order.

In next-to-leading order the operators mix under renormalization with each other. Thus the evolution of $\langle 0|O_n(Q^2)|P\rangle^{\text{red}}$ is determined by an infinite coupled first-order differential equation system. Since the anomalous dimension matrix is triangular, this system can be perturbatively solved, resulting in a behavior qualitatively different than the solution from leading order.

For instance, if the initial condition is set as $\varphi(x, Q_0^2) = \varphi^{as}(x) = 6(1-x)x$ at the reference momentum square Q_0^2 , then all higher harmonics will also be excited. In the limit $Q^2 \rightarrow \infty$, these excitations disappear, returning to $\varphi^{as}(x)$. This effect is investigated more generally and quantitatively in the following two sections.

3 Next to Leading Analysis for Fixed Coupling Constant

To see the essential features of the next-to-leading-order correction, consider first the solution of the evolution equation for fixed coupling constant α_s . In this case, the mentioned excitation of higher harmonics by evolution will not disappear in the asymptotic limit $Q^2 \rightarrow \infty$. Expansion of $\varphi(x, Q^2)$ with respect to the eigenfunctions $\varphi_n^{ef}(x, \alpha_s)$ of the evolution kernel $V(x, y, \alpha_s)$ provides immediately the solution of the evolution equation:

$$\varphi(x, Q^2) = \sum_{n=0}^{\infty} \varphi_n^{ef}(x, \alpha_s) \left(\frac{Q^2}{Q_0^2}\right)^{\gamma_n(\alpha_s)/2} \langle 0|O_n(Q_0^2)|P\rangle^{\text{red}}. \quad (10)$$

The next-to-leading-order corrections to the evolution enters as a two-loop contribution of the eigenvalues $\gamma_n(\alpha_s)/2$ and as α_s corrections to the eigenfunctions $\varphi_n^{ef}(x, \alpha_s)$. The two-loop corrections of the eigenvalues are well known from the next-to-leading-order analysis of deep inelastic scattering [29]. A closed expression for the α_s corrections to the eigenfunctions can be derived from conformal constraints and a one-loop calculation of the special conformal anomaly in Ref. [23] (Here, the result is re-expressed by a linear combination of Lerch transcendent $\phi[x, 1, i]$, and taking into account the term proportional to β_0 .),

$$\varphi_n^{ef}(x, \alpha_s) = (-1)^n \frac{2(3+2n)}{(n+1)!} \frac{d^n}{dx^n} x^{1+n} (1-x)^{1+n} \left(1 + \frac{\alpha_s}{2\pi} F_n(x) + O(\alpha_s^2)\right), \quad (11)$$

where

$$\begin{aligned}
F_n(x) &= -(\gamma_n^{(0)} - \beta_0) \left[\frac{1}{2} \ln(x(1-x)) - \psi(2+n) + \psi(4+2n) \right] \\
&+ C_F \left[\frac{\ln^2\left(\frac{1-x}{x}\right)}{2} - \sum_{i=1}^{1+n} \left(-\frac{1}{i} + \frac{1+\delta_{0n}}{2+n} \right) (\phi(1-x, 1, i) + \phi(x, 1, i)) \right. \\
&\quad \left. + 2 \left(\frac{(3+2n)(\gamma_E + \psi(2+n))}{(1+n)(2+n)} + \psi'(2+n) - \frac{\pi^2}{4} \right) \right], \quad (12)
\end{aligned}$$

where $\psi(z) = d \ln(\Gamma[z])/dz$, $\gamma_E = 0.5772, \dots$, and $\phi(x, 1, i) = \sum_{k=0}^{\infty} x^k/(i+k)$. The term proportional to $\gamma_n^{(0)}$ in Eq. (12) can be obtained directly by assuming a nontrivial fixpoint α_s^* , i.e., $\beta(\alpha_s^*) = 0$, from a conformal operator product expansion [31]. I thus refer to it as conformal symmetry predicted part. Conformal symmetry breaking by the β -function provides a shift of the anomalous dimensions $\gamma_n^{(0)} \rightarrow \gamma_n^{(0)} - \beta_0$. The remaining term in Eq. (12) is proportional to the color factor C_F , and can be interpreted as an ‘additional’ conformal symmetry breaking term that comes from the renormalization of the conformal operators in gauge field theory.

3.1 Corrections to the eigenfunctions

Consider the asymptotic limit $Q^2 \rightarrow \infty$. As in leading order, the asymptotic distribution amplitude is completely determined by the eigenfunction φ_0^{ef}

$$\begin{aligned}
\varphi_0^{as}(x, \alpha_s) &= \varphi_0^{ef}(x, \alpha_s), \\
&= 6(1-x)x \left(1 + \frac{\alpha_s}{4\pi} \left\{ C_F \left[\ln^2\left(\frac{1-x}{x}\right) + 2 - \frac{\pi^2}{3} \right] + \beta_0 \left[\ln\left((1-x)x\right) + \frac{5}{3} \right] \right\} \right) \quad (13)
\end{aligned}$$

The term in φ_0^{ef} proportional to β_0 , gives a logarithmic modification. It is very interesting that the conformal symmetry breaking term provides an unexpected \ln^2 modification of the endpoint behavior. The α_s correction to the asymptotic distribution amplitude (13) is shown in Figs. 2(a,b).

We next study quantitatively the α_s contributions for the eigenfunctions with arbitrary n . For this purpose, it is technically more convenient to deal with the following representation [23]:

$$\begin{aligned}
\varphi_n^{ef}(x, \alpha_s) &= \frac{(1-x)x}{N_n} C_n^{3/2}(2x-1) + \frac{\alpha_s}{2\pi} \varphi_n^{ef(1)}(x) + O(\alpha_s^2), \\
\varphi_n^{ef(1)}(x) &= \sum_{k=n+2}^{\infty} \frac{(1-x)x}{N_k} C_k^{3/2}(2x-1) c_{kn}^{(1)}, \quad (14)
\end{aligned}$$

where

$$c_{kn}^{(1)} = \frac{(2n+3)(\gamma_n^{(0)} - \beta_0 + 4A_{kn})}{(k-n)(k+n+3)} + \frac{2(2n+3)(A_{kn} - \psi(k+2) + \psi(1))}{(n+1)(n+2)},$$

and

$$A_{kn} = C_F \left[\psi\left(\frac{k+n+4}{2}\right) - \psi\left(\frac{k-n}{2}\right) + 2\psi(k-n) - \psi(k+2) - \psi(1) \right] \quad (15)$$

are only nonzero if $k-n$ even. To comprehend these α_s contributions quantitatively, consider the amplitude at $x = 0.5$. However, since the $\ln^2((1-x)/x)$ term in Eq. (13) disappears at $x = 0.5$, it is clear that the large contributions of the endpoint region will be dropped out. Nevertheless, from Eq. (14) and $C_{2n}^{3/2}(0) = (-1)^{(n)} \Gamma(3/2+n) / (\Gamma(1+n) \Gamma(3/2))$ [30], the relative contributions $r_n^{(1)} = \varphi_n^{(1)ef}(0.5) / \varphi_n^{(0)ef}(0.5)$ increase logarithmically with n , and are of order 2 for $n = 10$ ($\beta_0 = 0$), respectively, for $n = 2$ ($\beta_0 = 9$).

To take into account the missed logarithmic modification in the endpoint behavior, it is more reasonable to use the following quantitative measure for the $O(\alpha_s)$ contribution:

$$R_n(\alpha_s) = \left(\int_0^1 \frac{N_n \varphi_n^{ef}(x, \alpha_s)^2}{(1-x)x} - 1 \right)^{1/2} = \frac{\alpha_s}{2\pi} R_n^{(1)} + O(\alpha_s^2). \quad (16)$$

Figure 1(a,b) shows that this analysis provides qualitatively the same n -dependence as for $r_n^{(1)}$, and that the α_s contributions are now larger. Moreover, the following are common features of the α_s corrections to the eigenfunctions:

- For $n = 0$ and $\beta_0 = 0$, only the ‘additional’ conformal symmetry breaking part gives a contribution, of order $\alpha_s/2\pi$. For $\beta_0 \neq 0$, this term is partly cancelled.
- Contributions from the symmetry predicted and breaking parts have different phases, so that the net-contribution is smaller.
- In the case of $\beta_0 = 0$, the minimum is at $n=6$. For $\beta_0 \neq 0$, this effect is washed out. For small n and $\beta_0 = 0$, the corrections are small.
- The relative corrections are growing logarithmically,
 $r_n^{(1)} \sim 0.347\beta_0 - (2.71 + 1.39 \ln(2+n)) C_F$,

$$R_n^{(1)} \sim \left[0.411\beta_0^2 + (54.7 - 35.9 \ln(2+n) + 6.58 \ln^2(2+n)) C_F^2 + (-8.98 + 3.29 \ln(2+n)) \beta_0 C_F \right]^{(1/2)},$$

and in the limit $n \rightarrow \infty$, the relative corrections are independent of β_0 .

Later, the evolution of $\varphi(x, Q^2)$ will be computed numerically. For this purpose, it is necessary to know how well the partial sums

$$\varphi_{ni}^{ef(1)}(x) = \sum_{k=n+2}^{n+2i} \frac{(1-x)x}{N_k} C_k^{3/2}(2x-1) c_{kn}^{(1)} \quad (17)$$

approximate the functional series (14). This is also important for the case of running coupling, where the partial waves beyond the leading order are given by the functional series that have convergence properties similar to the series for the eigenfunctions. The relative deviation from $\varphi_n^{ef(1)}(x)$ can be measured by

$$\Delta_{ni} = \sqrt{1 - \frac{\int_0^1 dx \varphi_{ni}^{ef(1)}(x)^2 / (x(1-x))}{\int_0^1 dx \varphi_n^{ef(1)}(x)^2 / (x(1-x))}}, \quad \int_0^1 dx \frac{\varphi_{ni}^{ef(1)}(x)^2}{x(1-x)} = \sum_{k=n+2}^{n+2i} \frac{(C_{kn}^{(1)})^2}{N_k}. \quad (18)$$

Numerical computation shows that for $n = 0$, where $\beta_0 = 0$, the deviation is 43% for $i = 1$, about 10% for $i = 5$, and about 1% for $i = 21$. In general, to get the same deviation for $n > 0$, a larger number of terms is taken into account; e.g., for $n = 4$ the deviation is 50% for $i = 5$, 10% for $i = 19$, and 1% for $i = 82$. In Figs. 1(c,d), the n -dependence of the deviation is shown for the cases that keep (c) two terms and (d) ten terms of the expansion (17). To remain under the 3% level for $n \leq 500$ it is necessary to keep 50 terms. The asymptotic expansion of Δ_{ni} for large i and n , where $i \ll n$,

$$\Delta_{ni} \simeq \sqrt{\frac{1}{1+i}} \sqrt{\frac{\left(0.5 - \frac{2C_F [2.96 + \ln(1+i)]}{\beta_0 - C_F [0.692 - 4 \ln(2+n)]}\right)^2}{0.411 + \frac{48.7C_F^2 - 8.42C_F [\beta_0 - C_F [0.692 - 4 \ln(2+n)]]}{(\beta_0 - C_F [0.692 - 4 \ln(2+n)])^2}}} + \dots \quad (19)$$

is proportional to $1/\sqrt{1+i}$ for fixed n . Furthermore, Δ_{ni} increases with n and has the limit $\lim_{n \rightarrow \infty} \Delta_{ni} \simeq 0.78/\sqrt{1+i}$. In this limit there are much larger values when n is moderately large; e.g., $n \sim 100$:

$$\lim_{n \rightarrow \infty} \Delta_{n2} \simeq 0.49, \quad \lim_{n \rightarrow \infty} \Delta_{n10} \simeq 0.235, \quad \lim_{n \rightarrow \infty} \Delta_{n50} \simeq 0.11, \quad \lim_{n \rightarrow \infty} \Delta_{n5000} \simeq 0.011. \quad (20)$$

To approximate the logarithmic endpoint behavior of $\varphi_n^{ef}(x, \alpha_s)$, a much larger number of terms than suggested from the previous analysis should be taken into account. For situations where the endpoint behavior is crucial, e.g., for the next-to-leading-order analysis of the elastic pion form factor, it is better to use the following integral representation [23]:

$$\varphi_n^{ef}(x, \alpha_s) = \int_0^1 dy \left(\delta(x-y) + \frac{\alpha_s}{2\pi} c^{(1)}(x, y) + \dots \right) \frac{(1-y)y}{N_n} C_n^{3/2}(2y-1), \quad (21)$$

where

$$c^{(1)}(x, y) = (I - \mathcal{P}) \left(\frac{\beta_0}{2} S(x, y) - \int_0^1 dz S(x, z) V^{(0)}(z, y) + [g(x, y)]_+ \right),$$

$$[g(x, y)]_+ = g(x, y) - \delta(x-y) \int_0^1 dz g(z, y),$$

$$g(x, y) = C_F \theta(y-x) \frac{\ln\left(1 - \frac{x}{y}\right)}{(x-y)} + \left\{ \begin{array}{l} x \rightarrow 1-x \\ y \rightarrow 1-y \end{array} \right\}. \quad (22)$$

Furthermore, the convolution with the kernel $S(x, y)$ generates a shift of the Gegenbauer polynomial order

$$\int_0^1 dy S(x, y) \frac{(1-y)y}{N_n} C_n^{3/2}(2y-1) = \frac{d}{d\rho} \frac{((1-x)x)^{1+\rho}}{N_n} C_n^{3/2+\rho}(2x-1) \Big|_{\rho=0}, \quad (23)$$

and the operator \mathcal{P} projects on the diagonal part of the expansion of a function $f(x, y)$ with respect to $C_i^{3/2}$; i.e., $\mathcal{P}f(x, y) = \sum_{i=0}^{\infty} (1-x)x/N_i C_i^{3/2}(2x-1) f_{ii} C_i^{3/2}(2y-1)$, where f_{ij} with $0 \leq i, j \leq \infty$ are the expansion coefficients. Although the operator \mathcal{P} and the kernel $S(x, y)$ are only defined implicitly, Eq. (22) is nevertheless helpful to convolute $c^{(1)}(x, y)$ with a given hard scattering amplitude.

Finally, from Eq. (21), the α_s corrections to the eigenfunctions can be written as convolution

$$\delta^{ef} \varphi(x, Q^2) = \frac{\alpha_s}{2\pi} \int_0^1 dy \left(c^{(1)}(x, y) + \dots \right) \varphi^d(y, Q^2), \quad (24)$$

where the partial waves of $\varphi^d(x, Q^2)$ are given as Gegenbauer polynomials

$$\varphi^d(x, Q^2) = \sum_{n=0}^{\infty} \frac{(1-x)x}{N_n} C_n^{3/2}(2x-1) \left(\frac{Q^2}{Q_0^2} \right)^{\gamma_n(\alpha_s)/2} \langle 0 | O_n(Q_0^2) | P \rangle^{\text{red}}. \quad (25)$$

A further advantage of the representation (24) is that the above mentioned excitation of higher harmonics is now completely included in the kernel $c^{(1)}(x, y)$.

3.2 Corrections to the eigenvalues

The two-loop corrections to the anomalous dimensions $\gamma_n(\alpha_s)$ are given in Ref. [29]. As in one-loop order $\gamma_n^{(1)} < 0$ for all $n > 0$ holds true. Thus, if these two-loop corrections are resummed in

$$(Q/Q_0) \left(\alpha_s/2\pi \right) \gamma_n^{(0)} + (\alpha_s/2\pi)^2 \gamma_n^{(1)},$$

the (modified) partial waves for $n > 0$ will be more strongly suppressed than in leading order. The relative two-loop corrections to $\gamma_n(\alpha_s)$ are about $4.5\alpha_s/(2\pi)$ [$4\alpha_s/(2\pi)$] for all $n > 0$ and $n_f = 3$ [$n_f = 4$], giving a correction of 20% for reliable values of $\alpha_s \sim 0.35$. The relative correction to the evolution of the distribution amplitude is probably of the same order. (This kind of correction does not appear directly in the evolution of the asymptotic distribution amplitude, so that in this case they are much smaller.)

If the corrections arising from the eigenvalues are expanded with respect to α_s , it is possible to write these corrections as convolution with the leading order solution of the evolution equation,

$$\delta^{ev} \varphi(x, Q^2) = \left(\frac{\alpha_s}{2\pi} \right)^2 \ln \left(\frac{Q^2}{Q_0^2} \right) \int_0^1 dy V^{d(1)}(x, y) \varphi^{LO}(y, Q^2) \quad (26)$$

where $V^{d(1)}(x, y) = \mathcal{P}V^{(1)}(x, y)$ is the diagonal part of $V^{(1)}(x, y)$.

Although the kernel $V^{(1)}(x, y)$ is known in a closed form, it seems a more difficult task to extract the diagonal part $V^{d(1)}(x, y)$. A reasonable approximation can be found from the fact that $\gamma_n^{(1)}$ grows like $\gamma_n^{(0)}$, i.e., only logarithmically, for increasing n . The simple form of the asymptotic expansion

$$\begin{aligned}\gamma_n^{as(0)} &\simeq -5.3333 \ln(2+n) + 0.9215, \\ \gamma_n^{as(1)} &\simeq -(33.237 - 2.963n_f) \ln(2+n) + 15.315 - 1.4363n_f,\end{aligned}\quad (27)$$

and the eigenvalue equation [which is known from the one-loop approximation of $V(x, y)$]

$$\begin{aligned}\int_0^1 dy [v_b(x, y)]_+ (1-y)y C_n^{3/2}(2y-1) &= 2(1 - \gamma_E - \psi(n+2)) (1-x)x C_n^{3/2}(2x-1), \\ [v_b(x, y)]_+ &= v_b(x, y) - \delta(x-y) \int_0^1 dz v_b(z, y),\end{aligned}\quad (28)$$

$$v_b(x, y) = \theta(y-x) \frac{x}{y(y-x)} + \left\{ \begin{array}{l} x \rightarrow 1-x \\ y \rightarrow 1-y \end{array} \right\},$$

where $\psi(n+2) = \ln(n+2) + O(1/n)$ for large n , allows us to reexpress Eq. (26) as

$$\delta^{ev} \varphi(x, Q^2) = \left(\frac{\alpha_s}{2\pi}\right)^2 \ln\left(\frac{Q^2}{Q_0^2}\right) \left[\int_0^1 dy (a\delta(x-y) + b[v_b(x, y)]_+) \varphi^{LO}(y, Q^2) + R(x, Q^2) \right], \quad (29)$$

where $a \simeq 0.6315 - 0.0918n_f$ and $b \simeq 8.309 - 0.7408n_f$. The terms in the sum representation of the remainder

$$\begin{aligned}R(x, Q^2) &= \int_0^1 dy (V^{d(1)}(x, y) - a\delta(x-y) - b[v_b(x, y)]_+) \varphi^{LO}(y, Q^2), \\ &= \frac{1}{2} \sum_{n=0}^{\infty} \frac{(1-x)x}{N_n} C_n^{3/2}(2x-1) (\gamma_n^{(1)} - \gamma_n^{as(1)}) \left(\frac{Q^2}{Q_0^2}\right)^{\alpha_s \gamma_n^{(0)}/(4\pi)} \langle 0|O_n(Q_0^2)|P \rangle^{\text{red}}\end{aligned}\quad (30)$$

are additionally suppressed by $O(1/n)$. Thus, for the same accuracy, the approximation of $R(x, Q^2)$ by a partial sum requires less terms than the approximation of $\varphi^{LO}(y, Q^2)$ itself.

3.3 Complete next-to-leading order corrections

In the asymptotic limit, each given distribution amplitude $\varphi(x, Q_0^2)$ at reference momentum square Q_0^2 extends into the asymptotic distribution amplitude (13). Thus, in this limit, the relative next-to-leading-order correction $[\varphi^{NLO}(x) - \varphi^{LO}(x)]/\varphi^{LO}(x)$ is uniquely given by

$$\frac{\varphi^{asNLO}(x) - \varphi^{asLO}(x)}{\varphi^{asLO}(x)} = \frac{\alpha_s}{4\pi} \left(C_F \left[\ln^2\left(\frac{1-x}{x}\right) + 2 - \frac{\pi^2}{3} \right] + \beta_0 \left[\ln\left((1-x)x\right) + \frac{5}{3} \right] \right), \quad (31)$$

so it is large and enhanced in the endpoint region. The next-to-leading-order contribution by the evolution of the distribution amplitude is also important away from this asymptotic limit.

It is possible to get information about the distribution amplitude at low momentum transfer; e.g., $Q_0 \sim 0.5$ GeV, from nonperturbative methods such as sum rules [32] and lattice calculation [33]. However, the obtained results are inconclusive, so it is not possible to distinguish between the following parameterizations:

$$\begin{aligned}
\varphi^{as}(x) &= 6x(1-x) , \\
\varphi^{CZ}(x) &= 30x(1-x) \left(1 - 4x(1-x)\right) , \\
\varphi^{co}(x) &= \frac{8}{\pi} \left(x(1-x)\right)^{1/2} .
\end{aligned} \tag{32}$$

The function $\varphi^{co}(x)$ which was used for the next-to-leading-order analyses of the pion form factor in Ref. [17] is only one example of further convex amplitudes. (For a numerical calculation, $\varphi^{co}(x)$ is more suitable than broader amplitudes, which had previously been assumed to be more realistic.) Furthermore, it is assumed that the evolution of $\varphi(x, Q^2)$ for $Q > 0.5$ GeV can be obtained from the perturbative solution of the evolution equation.

The evolution of $\varphi(x, Q^2)$ is controlled by Eq. (10), where the reduced expectation values $\langle 0|O_n(Q_0^2)|P \rangle^{\text{red}}$ are computed from the nonperturbative input $\varphi(x, Q_0^2)$, which is assumed to be one of the functions in Eq. (32). It follows from Eqs. (10) and (14) up to corrections of order $O(\alpha_s^2)$,

$$\begin{aligned}
\langle 0|O_n(Q_0^2)|P \rangle^{\text{red}} &= m_n(Q_0^2) - \frac{\alpha_s}{2\pi} \sum_{i=0}^{n-2} c_{ni}^{(1)} m_i(Q_0^2) , \\
m_n(Q_0^2) &= \int_0^1 dx C_n^{3/2}(2x-1) \varphi(x, Q_0^2) ,
\end{aligned} \tag{33}$$

where the coefficients $c_{ni}^{(1)}$ are defined in Eq. (15).

Taking into account a sufficient number of terms in the series (10), the distribution amplitude at the factorization scale for exclusive processes assumed to be $Q \sim 2$ GeV can be obtained numerically. The number of active flavors is three, and the value for the fixed coupling constant is $\alpha_s = 0.5$. The distribution amplitude was approximated by the first 100 nontrivial terms ($i = 0, 2, \dots, 200$). The corresponding eigenfunctions $\varphi_n^{ef}(x, \alpha_s)$ take into account the $(102 - i/2)$ terms of the expansions with respect to Gegenbauer polynomials. The distribution amplitude $\varphi(x_j, Q^2)$ at $Q = 2$ GeV was then computed for different points x_j , $j = 0, 1, \dots, 70$ and interpolated to a smooth function.

It can be seen in Figs. 2(b,c,d) that the relative next-to-leading-order corrections have the following features:

- Independent of the shape of $\varphi(x, Q_0)$, the relative next-to-leading-order corrections are characterized by logarithmic enhancement at the endpoints caused by both corrections to the eigenfunctions and to the eigenvalues.
- For partial waves with $n > 0$, the corrections coming from the eigenvalues are larger than from the eigenfunctions. However, these corrections disappear in the asymptotic limit.

- Amplitudes enhanced at the endpoints, also have larger relative next-to-leading-order corrections that are negative.

Although it was possible for the chosen distribution amplitudes to compute the evolution in next-to-leading-order numerically, this will be a difficult task for amplitudes that are broader. In addition, the complete next-to-leading-order analyses for an exclusive process can be done more conveniently if the next-to-leading-order correction is written as a convolution, with the distribution amplitude $\varphi^d(x, Q^2)$ defined in Eq. (25), which also evolves smoothly in next-to-leading-order (no excitation of higher harmonics). Since $\varphi(x, Q^2) = \varphi^d(x, Q^2) + \delta^{ef} \varphi(x, Q^2)$ from Eq. (24),

$$\varphi(x, Q^2) = \int_0^1 dy \left(\delta(x-y) + \frac{\alpha_s}{2\pi} c^{(1)}(x, y) + \dots \right) \varphi^d(y, Q^2). \quad (34)$$

Again, the excitation of the higher partial waves is completely included in the convolution with $c^{(1)}(x, y)$. Notice that $\varphi^d(y, Q_0^2)$ may be used instead of $\varphi(y, Q_0^2)$ as an initial condition. In fact, this corresponds to the choice of another factorization scheme for the considered exclusive process (redefinition of the soft and hard parts).

The complete α_s correction to the evolution of the distribution amplitude in next-to-leading-order can easily be obtained from (24) and (26):

$$\begin{aligned} \varphi(x, Q^2) &= \varphi^{LO}(x, Q^2) + \delta^{ef} \varphi(x, Q^2) + \delta^{ev} \varphi(x, Q^2), \\ &= \int_0^1 dy \left(\delta(x-y) + \frac{\alpha_s}{2\pi} \left[c^{(1)}(x, y) + \frac{\alpha_s}{2\pi} \ln \left(\frac{Q^2}{Q_0^2} \right) V^{d(1)}(x, y) \right] + \dots \right) \varphi^{LO}(y, Q^2). \end{aligned} \quad (35)$$

4 Next-to-Leading-Order Analysis for Running Coupling Constant

This section discusses the solution of the evolution equation in next-to-leading-order for running coupling, which was derived in [23, 31],

$$\varphi(x, Q^2) = \sum_{n=0}^{\infty} \varphi_n(x, \alpha_s(Q^2)) \exp \left[\frac{1}{2} \int_{Q_0^2}^{Q^2} \frac{dt}{t} \gamma_n(g(t)) \right] \langle 0 | O_n(Q_0^2) | P \rangle^{\text{red}}. \quad (36)$$

The partial waves $\varphi_n(x, \alpha_s(Q^2))$ are now Q^2 dependent nonpolynomial functions, known as functional series

$$\begin{aligned} \varphi_n(x, \alpha_s(Q^2)) &= \frac{(1-x)x}{N_n} C_n^{\frac{3}{2}}(2x-1) + \frac{\alpha_s(Q^2)}{2\pi} \varphi_n^{(1)}(x, Q^2) + \dots, \\ \varphi_n^{(1)}(x, Q^2) &= \sum_{k=n+2}^{\infty} \frac{(1-x)x}{N_k} C_k^{\frac{3}{2}}(2x-1) s_{kn}(\alpha_s(Q^2)) c_{kn}^{(1)}, \end{aligned} \quad (37)$$

where $c_{kn}^{(1)}$ are the expansion coefficients of the eigenfunction defined in Eq. (15) and

$$s_{kn}(\alpha_s(Q^2)) = \frac{\gamma_k^{(0)} - \gamma_n^{(0)}}{\gamma_k^{(0)} - \gamma_n^{(0)} + \beta_0} \left[1 - \left(\frac{\alpha_s(Q_0^2)}{\alpha_s(Q^2)} \right) \right] + (\gamma_k^{(0)} - \gamma_n^{(0)}) / \beta_0. \quad (38)$$

Since these partial waves satisfy the convenient initial condition

$$\varphi_n(x, \alpha_s(Q_0^2)) = \frac{(1-x)x}{N_k} C_k^{3/2}(2x-1), \quad (39)$$

the expectation values $\langle 0|O_n(Q_0^2)|P \rangle^{\text{red}}$ can be now simpler computed as for fixed α_s

$$\langle 0|O_n(Q_0^2)|P \rangle^{\text{red}} = \int_0^1 dx C_n^{\frac{3}{2}}(2x-1) \varphi(x, Q_0^2). \quad (40)$$

Because of the asymptotic behavior of $\gamma_k^{(0)} = -4 \ln(k+2) + \dots$, $s_{kn}(\alpha_s(Q^2))$ approaches 1 for $k \gg n$ and $\alpha_s(Q_0^2) > \alpha_s(Q^2)$ [see Fig. 3(a)]. Consequently, the behavior of $\varphi_n^{(1)}(x, \alpha_s(Q^2))$ in the endpoint region is determined by $c_{kn}^{(1)}$; i.e., it has the same logarithmic modification as $\varphi_n^{ef(1)}(x)$.

To avoid this excitation of higher harmonics (Gegenbauer polynomials) by the evolution, a new distribution amplitude analogous to the case for the fixed coupling constant is introduced that satisfies a diagonal evolution equation (the corresponding evolution kernel has to be diagonal with respect to Gegenbauer polynomials). A formal representation for this transformation kernel was given in [24],

$$W = \int_0^\infty dt \exp\{-(\beta_0 - V^{(0)})t\} \otimes [(\mathcal{I} - \mathcal{P})V^{(1)}] \otimes \exp\{-V^{(0)}t\}, \quad (41)$$

but, as was pointed out, this representation cannot be used for explicit calculations. Hopefully, changing the factorization scheme for the exclusive process under consideration will allow us to factorize the process amplitude in terms of the desired diagonal distribution amplitude $\varphi^d(x, Q^2)$.

For the numerical study of the next-to-leading-order corrections, assume that the distribution amplitude at $Q_0 = 0.5$ GeV ($\Lambda^{(3)} = 0.4$ in next-to-leading-order; i.e., that $\alpha_s(Q_0^2) \sim 0.9$) can be parametrized by one of the functions in Eq. (32). The amplitudes are evolved to a scale $Q = 2$ GeV, where $\alpha_s(Q^2) \sim 0.3$. The number of active flavors is three, taking into account the first 100 nontrivial terms in the partial sums for both series (36) and (37) [the asymptotic (Chernyak-Zhitnitsky) distribution amplitude requires only 1 (2) term(s) in (36)]. The result in Figs. 3(b,c,d) shows that the relative next-to-leading-order corrections for running coupling have qualitative and quantitative features similar to those in the case of fixed coupling discussed in Section 3.3.

5 Summary and Conclusion

This paper has shown that the (relative) next-to-leading-order correction to the evolution of the pion distribution amplitude is rather large, especially in the endpoint region, and that in this region the negative corrections are larger for enhanced amplitudes. The α_s correction to the partial waves comes from the off-diagonal matrix elements of γ_{nk} ; it can be interpreted as excitation of higher harmonics (Gegenbauer polynomials) by evolution, and appears as $\ln(x(1-x))$ and $\ln^2(x/(1-x))$ terms. The two-loop contribution to the anomalous dimension γ_n is for $n > 0$ much larger than the off-diagonal matrix elements of γ_{nk} ; i.e., about 20%

of the one-loop approximation. However, the exponentiation of the two-loop contribution provides a larger suppression of the corresponding harmonic's as in leading order (expansion with respect to α_s provides a large (negative) excitation of the harmonics).

The obtained large next-to-leading-order correction seems to contradict a previous analysis [24], where it was found that this correction is rather small. The explanation for this discrepancy is that (1) only the first few expansion coefficients c_{nk} were taken into account, and (2) the authors looked only to the evolution of $\varphi(x, Q^2)$ at $x = 0.5$. Furthermore, the reference momentum chosen for use in Ref. [24] was $Q_0 = 10\Lambda^{(3)} = 1 \text{ GeV}$ in leading order; i.e., $\alpha_s(Q_0^2 = 1\text{GeV}^2) \sim 0.3$. Such a choice provides a much smaller next-to-leading-order correction for $Q_0 = 1.25\Lambda^{(3)}$ (because $\alpha_s(Q_0^2 = 1.25^2\Lambda^2) \sim 0.9$, perturbation theory should be valid for the evolution of the distribution amplitude). Using a popular parameterization at lower reference momentum (e.g., $Q_0 \sim 0.5 \text{ GeV}$) provides logarithmic correction, which should be included in the input amplitude at a higher reference momentum.

The question of whether to include an α_s suppressed logarithmic correction to the input amplitude $\varphi(x, Q_0^2)$ can be avoid by choosing a distribution amplitude that evolves smoothly, with no excitation of higher harmonics by evolution. The amplitude $\varphi^d(x, Q^2)$ satisfies an evolution equation where the corresponding evolution kernel $V^d(x, y)$ is diagonal with respect to Gegenbauer polynomials. Consequently, in such a factorization scheme, the contribution responsible for the mentioned excitation of higher harmonics is now included as the α_s correction to the hard scattering amplitude of the considered process.

Because of the size of the discovered correction and its dependence upon the input amplitude, the evolution of the distribution amplitude has to be included in the next-to-leading-order analysis of exclusive hard momentum processes. For large enough Q^2 , the Sudakov suppression can be neglected so that, using the known expressions for the hard scattering amplitudes of the pion transition form factor and the electromagnetic form factor, it should be straightforward to re-analyze the next-to-leading-order corrections for these processes. Because of the large number of Feynman diagrams, the α_s correction to the hard scattering amplitude for the $\gamma\gamma \rightarrow M^+M^-$ processes for the case of equal momentum sharing was only computed numerically. It should nevertheless be possible to estimate the size of the correction coming from the evolution of the distribution amplitude. A general next-to-leading-order analysis for arbitrary distribution amplitudes requires an analytical calculation of the hard scattering amplitude (448 diagrams).

Acknowledgments

For helpful discussions I am grateful to S. Brodsky, A. Brandenburg, T. Hyer, and O. Jacob. This work was supported in part by Department of Energy contract DE-AC03-76SF00515 (SLAC), and by Deutschen Akademischen Austauschdienst.

References

- [1] S. J. Brodsky and G. P. Lepage, Phys. Lett. **87B**, 359 (1979); Phys. Rev. Lett. **43**, 545 (1979); (E) **43**, 1625 (1979).

- [2] V. L. Chernyak and A. R. Zhitnitsky, JETP Lett. **25**, 510 (1977); V. L. Chernyak, A. R. Zhitnitsky, and V. G. Serbo, JETP Lett. **26**, 594 (1977).
- [3] A. V. Efremov and A.V. Radyushkin, Phys. Lett. **94B**, 245 (1980).
- [4] A. Duncan and A. H. Mueller, Phys. Rev. D **21**, 1636 (1980).
- [5] S. J. Brodsky and G. P. Lepage, in *Perturbative QCD*, edited by A. H. Mueller (World Scientific, Singapore, 1989); V. L. Chernyak, Nucl. Phys. B (Proc. Suppl.)**7B**, 297 (1989).
- [6] S. J. Brodsky and G P. Lepage, Phys. Rev. D **22**, 2157 (1980).
- [7] S. J. Brodsky, SLAC preprint SLAC-PUB-6356 (1993).
- [8] N. Isgur and C. H. Llewellyn Smith, Phys. Rev. Lett. **52**, 1080 (1984); Phys. Lett. **217B**, 535 (1989); Nucl. Phys. B **317**, 526 (1989).
- [9] A. V. Radyushkin, Acta Physica Polonica B **15**, 403 (1984); Nucl. Phys. A **532**, 141 (1991).
- [10] C.-R. Ji, A. F. Sill, and R. M. Lombard-Nelson, Phys. Rev. D **36**, 165 (1987); C.-R. Ji and F. Amiri, Phys. Rev. D **42**, 3764 (1990).
- [11] T. Huang and Q.-X. Shen, Z. Phys. C **50**, 139 (1991); A. Szczepaniak and L. Mankiewicz, Phys. Lett. B **266**, 153 (1991).
- [12] H.-N. Li and G. Sterman, Nucl. Phys. B **381**, 129 (1992).
- [13] R. Jakob and P. Kroll, Phys. Lett. B **315**, 463 (1993); Phys. Lett. B **319**, 545 (E) (1993).
- [14] F. Del Aguila and M. K. Chase, Nucl. Phys. B **193**, 517 (1981).
- [15] E. Braaten, Phys. Rev. D **28**, 524 (1983).
- [16] R. D. Field, R. Gupta, S. Otto, and L. Chang, Nucl. Phys. B **186**, 429 (1981).
- [17] F.-M. Dittes and A. V. Radyushkin, Yad. Fiz. **34**, 529 (1981) [Sov. J. Nucl. Phys. **34**, 293 (1981)].
- [18] B. Nizić, Phys. Rev. D **35**, 80 (1987).
- [19] A. V. Radyushkin and R. S. Khalmuradov, Yad. Fiz. **42**, 458 (1985) [Sov. J. Nucl. Phys. **42** (2), 289 (1985)].
- [20] E. Braaten and S.-M. Tse, Phys. Rev. D **35**, 2255 (1987).
- [21] F.-M. Dittes and A.V Radyushkin, Phys. Lett. **134B**, 359 (1984); M. H. Sarmadi, Phys. Lett. **143B**, 471 (1984); G. R. Katz, Phys. Rev. D **31**, 652 (1985); S. V. Mikhailov and A. V. Radyushkin, Nucl. Phys. B **254**, 89 (1985).

- [22] F.-M. Dittes, D. Müller, D. Robaschik, B. Geyer, and J. Hořejši, Phys. Lett. **209B**, 325 (1988); Fortschr. Physik **42**, 101–141 (1994).
- [23] D. Müller, Phys. Rev. D **49**, 2525 (1994).
- [24] S. V. Mikhailov and A. V. Radyushkin, Nucl. Phys. B **273**, 297 (1986).
- [25] E. P. Kadantseva, S. V. Mikhailov, and A. V. Radyushkin, Yad. Fiz. **44**, 507 (1986) [Sov. J. Nucl. Phys. **44** (2), 326 (1986)].
- [26] S. J. Brodsky, Y. Frishman, G. P. Lepage, and C. Sachrajda, Phys. Lett. **91B**, 239 (1980).
- [27] Yu. M. Makeenko, Yad. Fiz. **33**, 842 (1981) [Sov. J. Nucl. Phys. **33**, 440 (1981)]; Th. Ohrndorf, Nucl. Phys. B **198**, 26 (1982); N. S. Craigie, V. K. Dobrev, and I. T. Todorov, Ann. of Phys. **159**, 411 (1985).
- [28] H. Bateman and A. Erdélyi, *Higher Transcendental Functions*, Vol. II (McGraw-Hill, NY, 1953) p. 156.
- [29] E. G. Floratos, D. A. Ross, and C. T. Sachrajda, Nucl. Phys. B **129**, 66 (1977); (E) B **139**, 545 (1978); A. González-Arroyo, C. López, and F. J. Ynduráin, Nucl. Phys. B **153**, 161 (1979).
- [30] H. Bateman and A. Erdélyi, *ibid.*, p. 174.
- [31] S. J. Brodsky, P. Damgaard, Y. Frishman, and G. P. Lepage, Phys. Rev. D **33**, 1881 (1986).
- [32] V. L. Chernyak and A. R. Zhitnitsky, Phys. Rep. **112**, 173 (1984); V. M. Braun and I. E. Filyanov, Z. Phys. C–Particles and Fields **44**, 157 (1989); S. V. Mikhailov and A. Radyushkin, Sov. J. Nucl. Phys. **49**, 494 (1989); I. Halperin, Z. Phys. C–Particles and Fields **56**, 615 (1992).
- [33] G. Martinelli and C. T. Sachrajda, Phys. Lett. B **190**, 151 (1987); Nucl. Phys. B **306**, 865 (1988); T. A. DeGrand and R. D. Loft, Phys. Rev. D **38**, 954 (1988); D. Daniel, R. Gupta, and D. G. Richards, Phys. Rev. D **43**, 3715 (1991).

Captions

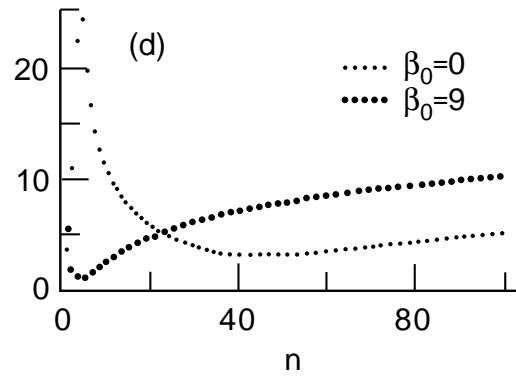
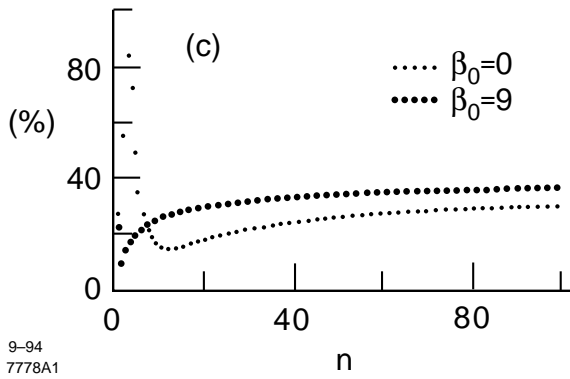
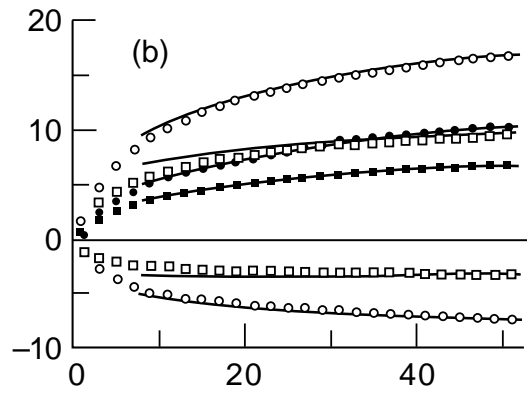
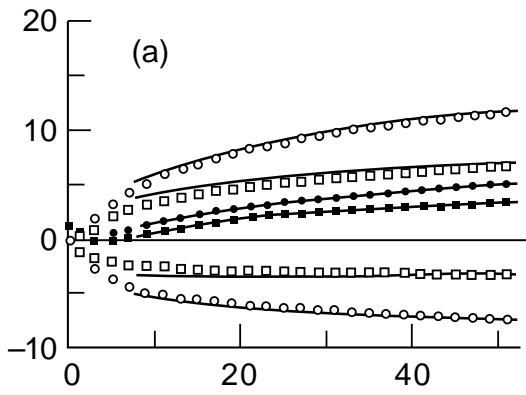
Fig. 1. Values of $r_n^{(1)}$ (boxes) and $R_n^{(1)}$ (circles) are given when (a) β_0 is set to zero, and (b) $\beta_0 = 9$. The difference of the relative value of the conformal symmetry predicted part (upper half plane) and of the relative value of the ‘additional’ conformal symmetry breaking term (lower half plane) is shown by filled boxes (circles). The lines represent the corresponding asymptotic expressions. (Subasymptotic terms were also taken into account for the approximation of $R_n^{(1)}$.) The relative deviation of the partial sums $\varphi_{nk}^{ef(1)}(x)$ from the exact α_s correction $\varphi_n^{ef(1)}(x)$ is given (c) for $k = 2$ and (d) for $k = 10$.

Fig. 2. Evolution of the pion distribution amplitude for fixed $\alpha_s = 0.5$ and three active flavors. As nonperturbative inputs, three distribution amplitudes defined in Eq. (32) are chosen at the reference momentum scale $Q_0 = 0.5$ GeV. They are shown in (a); $\varphi^{as}(x, Q^2)$ in leading order (solid), $\varphi^{CZ}(x, Q^2)$ (dashed), $\varphi^{co}(x, Q^2)$ (dash-dotted), $\varphi^{as}(x, Q^2)$ in next-to-leading-order (dotted). The relative next-to-leading-order corrections at $Q = 2$ GeV are shown for $\varphi^{as}(x, Q^2)$ in (b), for $\varphi^{CZ}(x, Q^2)$ in (c), and for $\varphi^{co}(x, Q^2)$ in (d) showing that the endpoint behavior of the distribution amplitudes changed more drastically under evolution. The next-to-leading-order corrections of the eigenvalues are neglected for the dashed line, expanded with respect to α_s for the dash-dotted line, and taken into account by resummation for the solid line. The correction in the asymptotic limit is dotted.

Fig. 3. The evolution of the pion distribution amplitude for running α_s is essentially determined by the matrix valued function $s_{kn}(\alpha_s(Q^2))$. (a) shows that $s_{kn}(\alpha_s(Q^2))$ defined in Eq. (38) as a function of $k/(n+2)$ is nearly n independent, and for $\alpha_s(Q^2) = 0.5\alpha_s(Q_0^2)$ it is almost of order $O(1)$. The relative next-to-leading-order corrections for $\varphi^{as}(x, Q^2)$ in (b), for $\varphi^{CZ}(x, Q^2)$ in (c), and for $\varphi^{co}(x, Q^2)$ in (d) are comparable to the fixed coupling result. Here, $\alpha_s(Q_0^2) = 0.9$, $\alpha_s(Q^2) = 0.3$, and three active flavors were chosen. The meaning of the solid, dashed, and dash-dotted lines is the same as for Fig. 2(b,c,d).

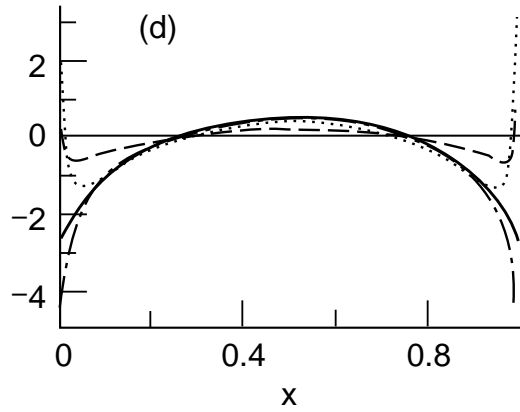
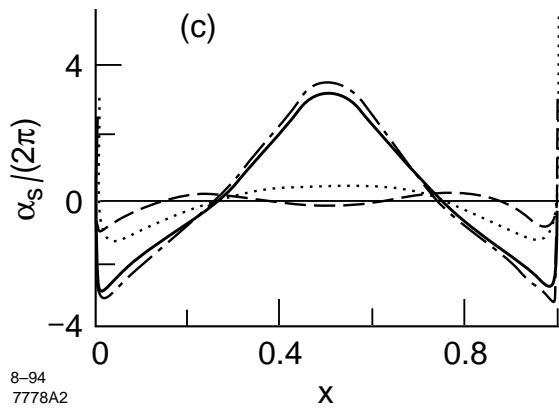
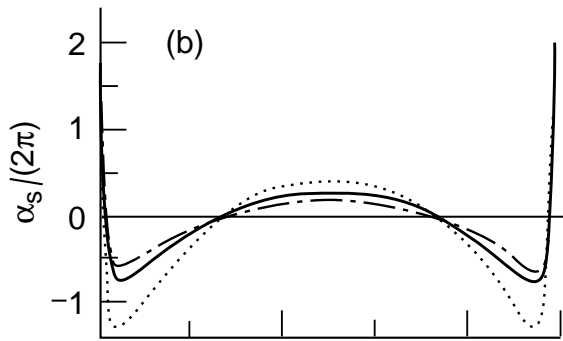
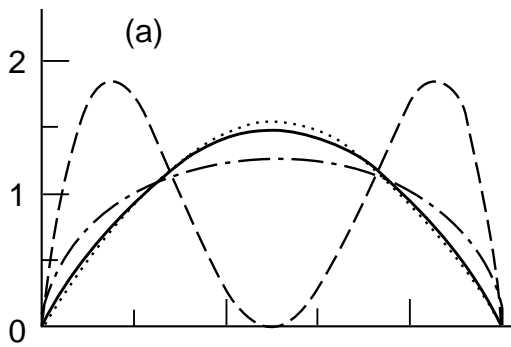
This figure "fig1-1.png" is available in "png" format from:

<http://arxiv.org/ps/hep-ph/9411338v1>



This figure "fig1-2.png" is available in "png" format from:

<http://arxiv.org/ps/hep-ph/9411338v1>



This figure "fig1-3.png" is available in "png" format from:

<http://arxiv.org/ps/hep-ph/9411338v1>

